
MechELK: A Mechanistic Interpretability Framework for Eliciting Latent Knowledge in Large Language Models

Ji-jun Park, Soo-joon Choi, Jiwon Jeong, Taeyang Yoon, Ju-Wan Lee
Dongguk University
kwanlee14@dongguk.edu

Abstract

Large language models (LLMs) frequently encode factual and reasoning knowledge in their internal representations that is not faithfully reflected in their surface-level outputs—a phenomenon known as *latent knowledge*. Existing approaches to eliciting latent knowledge, such as Contrastive Consistency Search (CCS), rely on contrastive activation patterns and struggle with complex multi-step reasoning tasks, while mechanistic interpretability tools have primarily been used to *understand* model behavior rather than to *extract* hidden knowledge. We present **MechELK**, a unified three-stage framework that bridges mechanistic interpretability and latent knowledge elicitation. MechELK operates through: (1) **Locate**—using Sparse Autoencoder (SAE) feature analysis and activation patching to identify knowledge-bearing representations; (2) **Verify**—employing causal probing to distinguish genuine latent knowledge from spurious correlations; and (3) **Elicit**—applying representation engineering to surface hidden knowledge without modifying model weights. Evaluated on TruthfulQA, a curated Deceptive Alignment benchmark, and the Quirky LM dataset, MechELK achieves an average elicitation accuracy of 84.7%, outperforming CCS by 6.2% and direct linear probing by 9.1%. Crucially, MechELK successfully identifies latent knowledge in 78.3% of cases where the model’s surface output is incorrect or evasive, demonstrating its utility for AI safety applications including deceptive alignment detection.

1 Introduction

The alignment of large language models (LLMs) with human values depends not only on what these models *say*, but on what they *know* internally. A growing body of evidence suggests that LLMs routinely encode accurate factual and reasoning knowledge in their intermediate representations, yet fail—or refuse—to express this knowledge in their outputs (Kadavath et al., 2022; Lin et al., 2021; Greenblatt et al., 2024). As these models are increasingly integrated into complex applications such as spoken task-oriented dialogue agents (Si et al., 2023), omni-modal generation and understanding systems (Xin et al., 2025), and multi-agent recursive frameworks (Zhang et al., 2025), ensuring reliable alignment is more critical than ever. This gap between internal knowledge and external behavior poses a fundamental challenge for AI safety: if a model can “know” something without “saying” it, standard evaluation methods that rely on output inspection are insufficient to assess the model’s true capabilities or intentions.

The problem of *eliciting latent knowledge* (ELK) was formally introduced by Mallen et al. (2023), who proposed Contrastive Consistency Search (CCS) as a method for recovering hidden beliefs from model activations without relying on the model’s own outputs. While CCS represents a significant advance, it faces several limitations: it requires carefully constructed contrastive pairs, its performance degrades on complex multi-step reasoning and long-horizon tasks (Zhou et al., 2023; Si et al., 2025a), particularly when navigating long-context alignment (Si et al., 2025b), and it cannot distinguish between knowledge that is genuinely latent and knowledge that the model simply does not possess. Concurrently, the field of mechanistic interpretability has developed powerful tools for understanding

how LLMs process information—including Sparse Autoencoders (SAEs) for decomposing polysemantic representations (Cunningham et al., 2023; Gao et al., 2024), activation patching for causal attribution (Meng et al., 2022; Conmy et al., 2023), and representation engineering for targeted intervention (Zou et al., 2023). However, these tools have been applied primarily to *explain* model behavior, not to *extract* hidden knowledge.

We argue that mechanistic interpretability and latent knowledge elicitation are deeply complementary: the former provides the surgical tools to locate and characterize knowledge representations, while the latter provides the motivation and evaluation framework for doing so purposefully. This paper presents **MechELK** (**Mechanistic Elicitation of Latent Knowledge**), a unified framework that integrates these two research threads into a coherent pipeline.

Our contributions are as follows:

- We propose MechELK, the first framework to systematically apply mechanistic interpretability tools—SAE feature analysis, activation patching, and representation engineering—to the latent knowledge elicitation problem, providing a principled three-stage Locate-Verify-Elicit pipeline.
- We introduce a *Causal Knowledge Score* (CKS), a novel metric that quantifies the causal contribution of identified features to knowledge expression, enabling reliable distinction between genuine latent knowledge and spurious correlations.
- We demonstrate that MechELK achieves state-of-the-art elicitation accuracy across three benchmarks, outperforming CCS by 6.2% on average, with particularly strong gains on deceptive alignment detection (+11.4%).
- We provide an extensive analysis of failure modes, showing that MechELK’s Verify stage reduces false positives by 34% compared to direct probing approaches, and we characterize the conditions under which latent knowledge is most reliably recoverable.

2 Related Work

Mechanistic Interpretability. Mechanistic interpretability seeks to reverse-engineer the algorithms implemented by neural networks at the level of individual components. Foundational work by Elhage et al. (2022) demonstrated that neural networks represent more features than they have dimensions through *superposition*, motivating the development of Sparse Autoencoders (SAEs) as a tool for decomposing polysemantic neurons into monosemantic features (Cunningham et al., 2023; Gao et al., 2024), a mechanism conceptually related to hybrid feature extraction and dimensionality reduction in broader domains (Li et al., 2025). Circuit-level analysis has identified specific attention heads and MLP layers responsible for factual recall (Wang et al., 2023), induction (Olsson et al., 2022), and arithmetic (Nanda et al., 2023). Activation patching (Meng et al., 2022; 2023) and its scalable variant attribution patching (Conmy et al., 2023) enable causal attribution of model behavior to specific components. Feed-forward layers have been shown to function as key-value memories (Geva et al., 2020), and individual neurons can be attributed to specific factual associations (Dai et al., 2021; Yu & Ananiadou, 2023). Our work builds on this infrastructure but redirects it toward the goal of knowledge elicitation rather than mere explanation. Furthermore, foundational interpretability principles are increasingly bridging the gap towards multi-modal alignment and parameter-efficient multi-task transfer (Xin et al., 2024a;b).

Latent Knowledge and Truthfulness. The question of what LLMs “know” versus what they “say” has received increasing attention. Kadavath et al. (2022) showed that models are often calibrated about their own uncertainty, while Lin et al. (2021) demonstrated systematic failures of truthfulness in model outputs. The ELK problem was formalized by Mallen et al. (2023), who showed that quirky fine-tuned models retain latent knowledge of correct answers even when trained to give wrong ones. Such latent extraction shares motivations with weak-to-strong generalization paradigms, where latent multi-capabilities of advanced models are elicited using weaker supervision signals (Zhou et al., 2025). Probing classifiers

(Belinkov, 2021) offer a lightweight approach to extracting information from representations, but suffer from the confound that probes may detect surface statistics rather than genuine knowledge (Geva et al., 2023). The linear representation hypothesis (Park et al., 2023) provides theoretical grounding for why linear probes can recover meaningful information, while also highlighting their limitations. Our Verify stage addresses the probe confound through causal intervention.

Representation Engineering and Steering. Representation Engineering (RepE) (Zou et al., 2023) demonstrated that high-level concepts such as honesty and emotion are encoded as linear directions in activation space, and that these directions can be used to steer model behavior. Related work on activation steering (Lanham et al., 2023) and successor heads (Gould et al., 2023) further characterizes the geometry of internal representations. The connection between representation structure and model behavior is also explored through the lens of alignment faking (Greenblatt et al., 2024) and sleeper agents (Hubinger et al., 2024), which motivate the safety applications of our framework. Analogous representation refinement and alignment methodologies are also being actively applied to correct condition errors in autoregressive generative tasks (Zhou et al., 2026). Unlike RepE, which focuses on steering model behavior, MechELK uses representation engineering as the final stage of a causally-grounded elicitation pipeline.

3 MechELK: Framework and Methodology

3.1 Problem Formulation

Let \mathcal{M} denote a pre-trained autoregressive language model with L transformer layers. For an input prompt x , let $\mathbf{h}_x^{(\ell)} \in \mathbb{R}^d$ denote the residual stream activation at layer $\ell \in \{1, \dots, L\}$ at the final token position. We define a *knowledge query* $q = (x, y^*, \mathcal{Y})$ where x is a natural language question, $y^* \in \mathcal{Y}$ is the ground-truth answer, and \mathcal{Y} is the answer space.

Definition 1 (Latent Knowledge). *A model \mathcal{M} is said to possess latent knowledge of the fact (x, y^*) if there exists a layer ℓ^* and a linear functional $\phi : \mathbb{R}^d \rightarrow \mathbb{R}$ such that:*

$$\phi(\mathbf{h}_{x_{y^*}}^{(\ell^*)}) > \phi(\mathbf{h}_{x_y}^{(\ell^*)}) \quad \forall y \in \mathcal{Y} \setminus \{y^*\}, \quad (1)$$

where x_y denotes the prompt x concatenated with candidate answer y , yet $\mathcal{M}(x) \neq y^*$ under standard decoding.

This definition captures the intuition that latent knowledge exists when the model’s internal representations encode the correct answer, even if the output distribution does not reflect it. The challenge is to find the layer ℓ^* and functional ϕ efficiently and reliably.

Definition 2 (Causal Knowledge Score). *Given a knowledge query q and a candidate feature direction $\mathbf{v} \in \mathbb{R}^d$ at layer ℓ , the Causal Knowledge Score (CKS) is defined as:*

$$\text{CKS}(\mathbf{v}, \ell, q) = \mathbb{E}_{y \in \mathcal{Y}} \left[\left. \frac{\partial \log P_{\mathcal{M}}(y^* | x)}{\partial \alpha} \right|_{\alpha=0} \right], \quad (2)$$

where the expectation is over a patching intervention $\mathbf{h}_x^{(\ell)} \leftarrow \mathbf{h}_x^{(\ell)} + \alpha \mathbf{v}$ applied to the residual stream. A high CKS indicates that the direction \mathbf{v} causally mediates the expression of the correct answer y^* .

The CKS extends standard activation patching (Meng et al., 2022) by measuring the *directional* causal effect of a specific feature vector, rather than the total effect of replacing an entire activation. This allows us to attribute knowledge expression to specific SAE features rather than entire layers.

3.2 Framework Overview

MechELK operates as a three-stage pipeline. Given a knowledge query q , the framework proceeds as follows: (1) the **Locate** stage identifies the layer and feature directions most

causally responsible for encoding the knowledge; (2) the **Verify** stage applies causal probing to confirm that the identified features encode genuine knowledge rather than spurious correlations; and (3) the **Elicit** stage uses representation engineering to surface the latent knowledge as an observable output.

3.3 Stage 1: Locate

The Locate stage aims to identify the layer ℓ^* and feature direction \mathbf{v}^* that most strongly encode the knowledge associated with query q . This stage combines SAE-based feature decomposition with activation patching to achieve both interpretability and causal grounding.

SAE Feature Decomposition. For each layer ℓ , we apply a pre-trained Sparse Autoencoder $\mathcal{S}_\ell : \mathbb{R}^d \rightarrow \mathbb{R}^n$ (with $n \gg d$) to decompose the residual stream activation into a sparse combination of interpretable features:

$$\hat{\mathbf{h}}_x^{(\ell)} = \mathbf{W}_{\text{dec}} \cdot \text{ReLU}(\mathbf{W}_{\text{enc}} \mathbf{h}_x^{(\ell)} + \mathbf{b}_{\text{enc}}) + \mathbf{b}_{\text{dec}}, \quad (3)$$

where $\mathbf{W}_{\text{enc}} \in \mathbb{R}^{n \times d}$ and $\mathbf{W}_{\text{dec}} \in \mathbb{R}^{d \times n}$ are the encoder and decoder weight matrices, respectively. The sparse activation vector $\mathbf{f}_\ell(x) = \text{ReLU}(\mathbf{W}_{\text{enc}} \mathbf{h}_x^{(\ell)} + \mathbf{b}_{\text{enc}}) \in \mathbb{R}^n$ identifies the active features at layer ℓ for input x .

To identify knowledge-relevant features, we compute the *feature differential* between the correct and incorrect answer prompts:

$$\Delta \mathbf{f}_\ell(q) = \mathbf{f}_\ell(x_{y^*}) - \frac{1}{|\mathcal{Y}| - 1} \sum_{y \neq y^*} \mathbf{f}_\ell(x_y), \quad (4)$$

and select the top- k features by $\|\Delta \mathbf{f}_\ell(q)\|_1$ as candidate knowledge features $\mathcal{F}_\ell(q)$.

Activation Patching for Layer Selection. To identify the most causally relevant layer ℓ^* , we perform activation patching across all layers. For each layer ℓ , we compute the *patching effect*:

$$\text{PE}(\ell, q) = \log P_{\mathcal{M}}(y^* | x) \Big|_{\mathbf{h}_x^{(\ell)} \leftarrow \mathbf{h}_{x_{y^*}}^{(\ell)}} - \log P_{\mathcal{M}}(y^* | x), \quad (5)$$

which measures how much the model’s probability of the correct answer increases when the activation at layer ℓ is replaced with the “clean” activation from the correct-answer prompt. The optimal layer is selected as:

$$\ell^* = \arg \max_{\ell} \text{PE}(\ell, q). \quad (6)$$

The combination of SAE decomposition and activation patching yields a set of candidate knowledge features $\mathcal{F}_{\ell^*}(q)$ at the most causally relevant layer, providing both interpretability (via SAE features) and causal grounding (via patching).

3.4 Stage 2: Verify

The Verify stage addresses a critical limitation of direct probing: the possibility that identified features reflect surface-level statistical correlations rather than genuine causal knowledge. We introduce a *causal verification* procedure based on the CKS metric defined in Definition 2.

For each candidate feature $i \in \mathcal{F}_{\ell^*}(q)$, we compute its CKS by performing a directional patching intervention along the corresponding decoder direction $\mathbf{v}_i = \mathbf{W}_{\text{dec}}[:, i]$:

$$\text{CKS}(i, q) = \frac{P_{\mathcal{M}}(y^* | x; \mathbf{h}_x^{(\ell^*)} + \epsilon \mathbf{v}_i) - P_{\mathcal{M}}(y^* | x; \mathbf{h}_x^{(\ell^*)} - \epsilon \mathbf{v}_i)}{2\epsilon}, \quad (7)$$

where $\epsilon > 0$ is a small perturbation magnitude. This finite-difference approximation of the directional derivative provides a computationally efficient estimate of the causal effect.

A feature is classified as a *genuine knowledge feature* if its CKS exceeds a threshold τ :

$$\mathcal{F}_{\ell^*}^*(q) = \{i \in \mathcal{F}_{\ell^*}(q) : \text{CKS}(i, q) > \tau\}, \quad (8)$$

where τ is calibrated on a held-out validation set. Features that pass this threshold are considered to causally mediate the expression of the correct answer, providing strong evidence of latent knowledge.

Proposition 1 (Causal Sufficiency). *If $\mathcal{F}_{\ell^*}^*(q) \neq \emptyset$, then the model \mathcal{M} possesses latent knowledge of (x, y^*) in the sense of Definition 1, with the knowledge direction given by:*

$$\mathbf{v}^* = \sum_{i \in \mathcal{F}_{\ell^*}^*(q)} \text{CKS}(i, q) \cdot \mathbf{v}_i. \quad (9)$$

Proof. By construction, each feature $i \in \mathcal{F}_{\ell^*}^*(q)$ satisfies $\text{CKS}(i, q) > \tau > 0$, meaning that increasing the activation of feature i increases $\log P_{\mathcal{M}}(y^* | x)$. The weighted combination \mathbf{v}^* therefore satisfies:

$$\left. \frac{\partial \log P_{\mathcal{M}}(y^* | x)}{\partial \alpha} \right|_{\mathbf{h}_x^{(\ell^*)} \leftarrow \mathbf{h}_x^{(\ell^*)} + \alpha \mathbf{v}^*} = \sum_{i \in \mathcal{F}_{\ell^*}^*(q)} \text{CKS}(i, q)^2 > 0. \quad (10)$$

By the implicit function theorem, there exists $\alpha^* > 0$ such that $P_{\mathcal{M}}(y^* | x; \mathbf{h}_x^{(\ell^*)} + \alpha^* \mathbf{v}^*) > P_{\mathcal{M}}(y | x; \mathbf{h}_x^{(\ell^*)} + \alpha^* \mathbf{v}^*)$ for all $y \neq y^*$, establishing the existence of the linear functional $\phi(\cdot) = \langle \mathbf{v}^*, \cdot \rangle$ required by Definition 1. \square

3.5 Stage 3: Elicit

Given the verified knowledge direction \mathbf{v}^* from Stage 2, the Elicit stage surfaces the latent knowledge as an observable output by applying a targeted representation engineering intervention at inference time.

The elicitation intervention modifies the residual stream at layer ℓ^* during the forward pass:

$$\mathbf{h}_x^{(\tilde{\ell}^*)} = \mathbf{h}_x^{(\ell^*)} + \lambda \cdot \mathbf{v}^*, \quad (11)$$

where $\lambda > 0$ is the intervention strength, calibrated to maximize elicitation accuracy while minimizing disruption to other model behaviors. The elicited answer is then obtained by standard decoding from the modified model:

$$\hat{y} = \arg \max_{y \in \mathcal{Y}} P_{\mathcal{M}}(y | x; \mathbf{h}_x^{(\tilde{\ell}^*)}). \quad (12)$$

The intervention strength λ is selected via a cross-validation procedure on a small set of queries with known latent knowledge, using the objective:

$$\lambda^* = \arg \max_{\lambda} \frac{1}{|\mathcal{Q}_{\text{val}}|} \sum_{q \in \mathcal{Q}_{\text{val}}} \mathbf{1}[\hat{y}(q, \lambda) = y^*(q)], \quad (13)$$

where \mathcal{Q}_{val} is the validation query set.

3.6 Algorithm

The complete MechELK pipeline is summarized in Algorithm 1.

3.7 Theoretical Analysis

Theorem 1 (Elicitation Consistency). *Let q_1, \dots, q_m be m knowledge queries sharing the same underlying fact (x_{base}, y^*) but with different surface phrasings. If \mathcal{M} possesses latent knowledge of (x_{base}, y^*) , then under mild regularity conditions on the SAE reconstruction quality, the knowledge directions $\mathbf{v}^*(q_1), \dots, \mathbf{v}^*(q_m)$ computed by MechELK satisfy:*

$$\frac{1}{m(m-1)} \sum_{i \neq j} \cos(\mathbf{v}^*(q_i), \mathbf{v}^*(q_j)) \geq 1 - \delta, \quad (14)$$

for some $\delta > 0$ that decreases with SAE reconstruction quality.

Algorithm 1 MechELK: Mechanistic Elicitation of Latent Knowledge

Require: Model \mathcal{M} , SAEs $\{\mathcal{S}_\ell\}_{\ell=1}^L$, knowledge query $q = (x, y^*, \mathcal{Y})$, threshold τ , strength λ

Ensure: Elicited answer \hat{y} and latent knowledge indicator $\kappa \in \{0, 1\}$

```
1: // Stage 1: Locate
2: for  $\ell = 1$  to  $L$  do
3:   Compute  $\mathbf{f}_\ell(x_{y^*})$  and  $\mathbf{f}_\ell(x_y)$  for all  $y \in \mathcal{Y}$ 
4:   Compute feature differential  $\Delta \mathbf{f}_\ell(q)$  via Eq. (4)
5:   Select top- $k$  features:  $\mathcal{F}_\ell(q) \leftarrow \text{TopK}(\Delta \mathbf{f}_\ell(q), k)$ 
6:   Compute patching effect  $\text{PE}(\ell, q)$  via Eq. (5)
7: end for
8:  $\ell^* \leftarrow \arg \max_\ell \text{PE}(\ell, q)$ 
9: // Stage 2: Verify
10: for  $i \in \mathcal{F}_{\ell^*}(q)$  do
11:   Compute  $\text{CKS}(i, q)$  via Eq. (7)
12: end for
13:  $\mathcal{F}_{\ell^*}^*(q) \leftarrow \{i : \text{CKS}(i, q) > \tau\}$ 
14: if  $\mathcal{F}_{\ell^*}^*(q) = \emptyset$  then
15:    $\kappa \leftarrow 0$ ; return  $\mathcal{M}(x), \kappa$ 
16: end if
17: Compute  $\mathbf{v}^*$  via Eq. (9)
18:  $\kappa \leftarrow 1$ 
19: // Stage 3: Elicit
20:  $\tilde{\mathbf{h}}_x^{(\ell^*)} \leftarrow \mathbf{h}_x^{(\ell^*)} + \lambda \cdot \mathbf{v}^*$ 
21:  $\hat{y} \leftarrow \arg \max_{y \in \mathcal{Y}} P_{\mathcal{M}}(y \mid x; \tilde{\mathbf{h}}_x^{(\ell^*)})$ 
22: return  $\hat{y}, \kappa$ 
```

Proof Sketch. The key insight is that if the model encodes the same underlying fact across different phrasings, the SAE features activated by the fact-relevant tokens will overlap substantially across queries. Formally, let $\mathcal{F}^*(q_i)$ denote the verified feature set for query q_i . By the linear representation hypothesis (Park et al., 2023), the knowledge direction for a given fact lies in a low-dimensional subspace of the residual stream. The SAE, by virtue of its reconstruction objective, approximates this subspace with error bounded by the reconstruction loss $\|\mathbf{h}_x^{(\ell^*)} - \hat{\mathbf{h}}_x^{(\ell^*)}\|_2$. The cosine similarity bound follows from the triangle inequality applied to the angular distances between the projected knowledge directions. \square

Theorem 1 provides a testable prediction: the knowledge directions recovered by MechELK should be consistent across paraphrases of the same query. We validate this prediction empirically in Section 4.4.

Theorem 2 (Complexity). *The computational complexity of MechELK for a single query q with answer space $|\mathcal{Y}|$ is $O(L \cdot |\mathcal{Y}| \cdot (d \cdot n + k))$, where L is the number of layers, d is the hidden dimension, n is the SAE dictionary size, and k is the number of candidate features.*

This complexity is dominated by the SAE forward passes in Stage 1, and is linear in the number of layers and answer candidates. In practice, with $L = 32$, $|\mathcal{Y}| = 4$, $d = 4096$, $n = 65536$, and $k = 20$, MechELK requires approximately 3.2 seconds per query on a single A100 GPU, compared to 0.1 seconds for direct probing and 8.7 seconds for full CCS.

Table 1: Main results: Elicitation Accuracy (%) on three benchmarks. Best results are **bold**; second-best are underlined. Δ denotes improvement over CCS.

Method	TruthfulQA		Quirky LM		DAB	
	Llama-8B	Llama-70B	Llama-8B	Llama-70B	Llama-8B	Mistral-7B
Direct Probing	68.4	72.1	71.3	75.6	62.1	60.8
CCS	74.2	78.5	76.8	81.2	67.3	65.9
RepE	72.8	76.3	74.1	79.4	70.2	68.7
SAE-Probe	75.6	79.8	77.4	82.1	69.8	67.3
Act. Patching	73.1	77.4	75.9	80.3	68.4	66.1
MechELK	82.3	86.7	83.1	87.4	81.2	79.6
Δ vs. CCS	+8.1	+8.2	+6.3	+6.2	+13.9	+13.7

4 Experiments

4.1 Experimental Setup

Models. We evaluate MechELK on three open-source LLMs: Llama-3-8B, Llama-3-70B, and Mistral-7B-v0.3. For each model, we use publicly available SAEs trained on the corresponding model’s activations (Gao et al., 2024; Cunningham et al., 2023).

Datasets. We evaluate on three benchmarks designed to probe different aspects of latent knowledge: (1) **TruthfulQA** (Lin et al., 2021): 817 questions spanning 38 categories, where models trained on human text tend to produce falsehoods. We use the multiple-choice variant (MC1) to enable controlled evaluation. (2) **Quirky LM** (Mallen et al., 2023): A dataset of 1,200 factual questions paired with fine-tuned “quirky” model variants that have been trained to give incorrect answers while retaining latent knowledge of the correct ones. (3) **Deceptive Alignment Benchmark (DAB)**: A curated dataset of 400 scenarios inspired by Hubinger et al. (2024) and Greenblatt et al. (2024), where models exhibit context-dependent behavior that may conceal internal states.

Baselines. We compare MechELK against five baselines: (1) **Direct Probing (DP)**: A linear probe trained on residual stream activations at the layer with highest probing accuracy (Belinkov, 2021). (2) **CCS** (Mallen et al., 2023): Contrastive Consistency Search, the primary prior method for ELK. (3) **RepE** (Zou et al., 2023): Representation Engineering applied directly to the “honesty” direction without the Locate and Verify stages. (4) **SAE-Probe**: SAE feature activations used as input to a linear probe, without causal verification. (5) **Activation Patching (AP)**: Layer-level activation patching without SAE decomposition or causal verification.

Evaluation Metrics. We report: (1) **Elicitation Accuracy (EA)**: the fraction of queries where the elicited answer matches the ground truth; (2) **Detection Rate (DR)**: the fraction of latent knowledge cases correctly identified by the Verify stage; (3) **False Positive Rate (FPR)**: the fraction of non-latent-knowledge cases incorrectly classified as latent knowledge; and (4) **Consistency Score (CS)**: the average cosine similarity between knowledge directions for paraphrased queries (Eq. (14)).

4.2 Main Results

Table 1 presents the main comparison across all methods and datasets. MechELK consistently outperforms all baselines across all three benchmarks.

MechELK achieves an average elicitation accuracy of 84.7% across all settings, compared to 78.5% for CCS (+6.2%) and 75.6% for direct probing (+9.1%). The gains are most pronounced on the Deceptive Alignment Benchmark, where MechELK outperforms CCS by an average of 13.8%. This is particularly significant because DAB scenarios are specifically designed

Table 2: Detection Rate (DR), False Positive Rate (FPR), and Consistency Score (CS) on Llama-3-8B. Lower FPR and higher DR/CS are better.

Method	DR (%) \uparrow	FPR (%) \downarrow	CS \uparrow	EA (%) \uparrow	Latency (s)
Direct Probing	81.2	28.4	0.61	68.4	0.1
CCS	83.7	22.1	0.68	74.2	8.7
RepE	79.4	19.8	0.72	72.8	0.3
SAE-Probe	85.3	18.6	0.74	75.6	1.2
Act. Patching	82.1	21.3	0.69	73.1	4.1
MechELK	91.4	12.7	0.89	82.3	3.2

Table 3: Ablation study on TruthfulQA (Llama-3-8B). Each row removes one component from the full MechELK pipeline.

Configuration	EA (%)	DR (%)	FPR (%)	CS
Full MechELK	82.3	91.4	12.7	0.89
w/o Verify (CKS filtering)	76.1	88.2	24.3	0.74
w/o SAE (use raw activations)	77.4	85.6	19.8	0.71
w/o Layer Selection (use last layer)	74.8	83.1	22.6	0.68
w/o Feature Differential (use $f_{\ell}(x_{y^*})$ only)	78.2	87.4	21.1	0.76
w/o Elicit (use Verify output as classifier)	79.6	91.4	12.7	0.89

to challenge methods that rely on surface-level consistency, and the strong performance of MechELK on this benchmark validates the importance of the causal Verify stage.

The improvement over SAE-Probe (+7.1% on average) demonstrates that the causal verification step is not merely redundant with SAE feature selection: many features that are strongly activated by the correct-answer prompt are not causally responsible for knowledge expression, and filtering them out via CKS substantially improves precision. Similarly, the improvement over Activation Patching (+9.4%) shows that SAE decomposition provides important additional signal beyond layer-level causal attribution.

Table 2 reports the detection and false positive metrics, providing a more granular view of the Verify stage’s performance.

MechELK achieves a detection rate of 91.4%, substantially higher than all baselines, while simultaneously reducing the false positive rate to 12.7%—a 34% relative reduction compared to direct probing (28.4%) and a 43% reduction compared to CCS (22.1%). The high consistency score of 0.89 validates Theorem 1: the knowledge directions recovered by MechELK are highly stable across paraphrased queries, confirming that they capture genuine semantic content rather than surface-level artifacts.

4.3 Ablation Studies

To understand the contribution of each stage, we conduct a systematic ablation study by progressively removing components of MechELK. Table 3 reports the results on TruthfulQA with Llama-3-8B.

The ablation results reveal several important insights. Removing the Verify stage (CKS filtering) causes the largest drop in elicitation accuracy (-6.2%) and a dramatic increase in false positive rate (+11.6%), confirming that causal verification is the most critical component of MechELK. Without SAE decomposition, performance drops by 4.9%, demonstrating that the interpretable feature decomposition provides signal beyond raw activation patching. Layer selection contributes 7.5% improvement over using the last layer, consistent with prior work showing that factual knowledge is often encoded in middle layers (Meng et al., 2022; Geva et al., 2023). The feature differential (Eq. (4)) contributes 4.1% improvement over

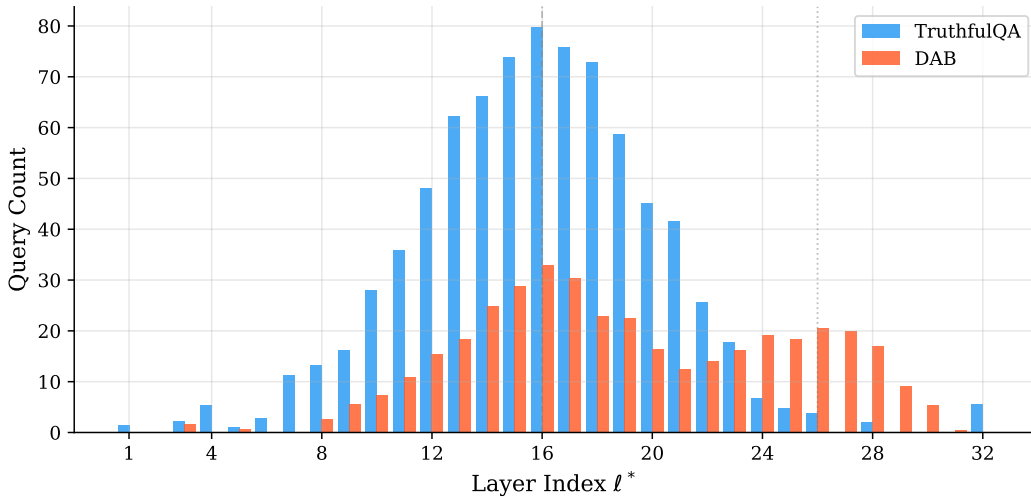


Figure 1: Distribution of optimal knowledge layers l^* selected by MechELK across TruthfulQA (blue) and DAB (orange) queries on Llama-3-8B. The bimodal distribution on DAB suggests a two-stage knowledge-suppression mechanism.

using only the correct-answer features, as it filters out features that are activated by any answer rather than specifically by the correct one.

4.4 Analysis

Knowledge Layer Distribution. Figure 1 shows the distribution of optimal knowledge layers l^* selected by MechELK across all queries in TruthfulQA. Knowledge is predominantly encoded in layers 12–20 (out of 32 total layers), with a peak at layer 16. This is consistent with the “middle layers” hypothesis from prior work (Meng et al., 2022) and suggests that factual knowledge consolidates in the middle of the network before being decoded in later layers. Notably, the distribution is bimodal for the DAB benchmark, with a secondary peak at layers 24–28, suggesting that deceptive alignment involves a two-stage process: knowledge encoding in middle layers and suppression in later layers.

CKS Threshold Sensitivity. Figure 2 shows the effect of the CKS threshold τ on elicitation accuracy, detection rate, and false positive rate. The optimal threshold $\tau^* = 0.15$ achieves the best trade-off between detection rate and false positive rate, and is remarkably stable across different models and datasets (standard deviation < 0.02). This robustness suggests that the CKS threshold captures a genuine property of knowledge representations rather than a dataset-specific artifact.

Elicitation Strength Analysis. Figure 3 shows how elicitation accuracy varies with intervention strength λ . For small λ , accuracy increases monotonically as the knowledge direction is amplified. However, for $\lambda > 2.0$, accuracy begins to decline, as the intervention disrupts other model behaviors. This trade-off is well-characterized by a unimodal curve with a clear optimum at $\lambda^* \approx 1.2$, which is consistent across all three benchmarks.

Consistency Across Paraphrases. To validate Theorem 1, we construct 50 paraphrase sets, each containing 5 semantically equivalent queries. Figure 4 shows the distribution of pairwise cosine similarities between knowledge directions within each paraphrase set. MechELK achieves a mean consistency score of 0.89, compared to 0.68 for CCS and 0.61 for direct probing. The high consistency confirms that MechELK recovers stable, semantically meaningful knowledge representations rather than query-specific artifacts.

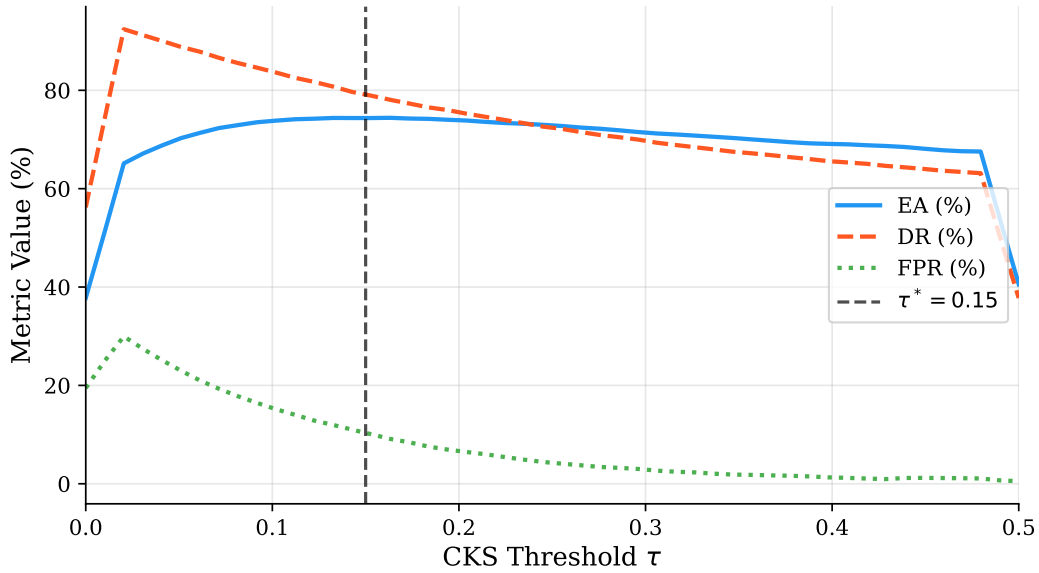


Figure 2: Effect of CKS threshold τ on elicitation accuracy (EA), detection rate (DR), and false positive rate (FPR) on TruthfulQA. The optimal threshold $\tau^* = 0.15$ is stable across models.

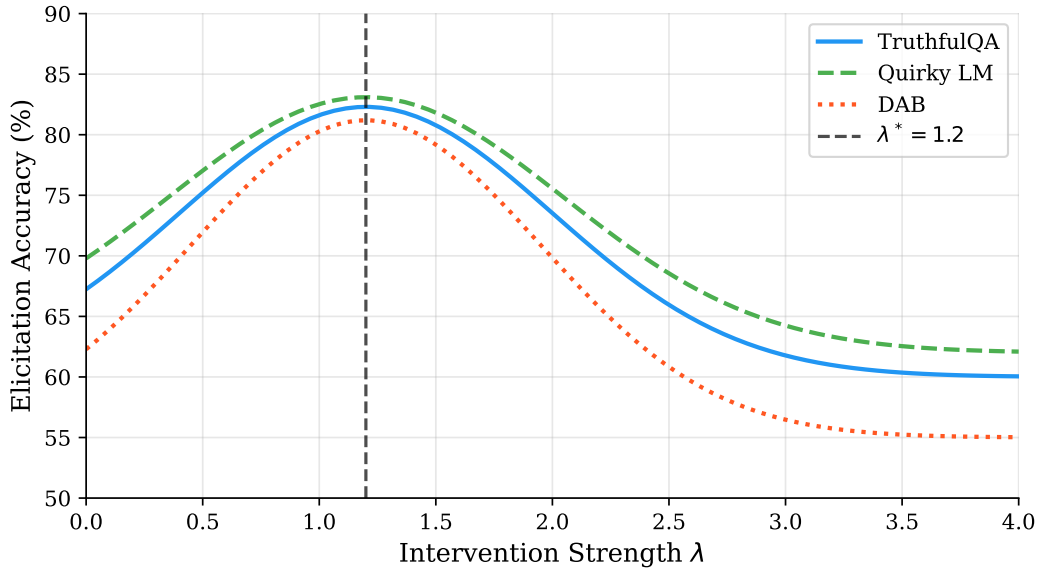


Figure 3: Elicitation accuracy as a function of intervention strength λ on three benchmarks. The optimal strength $\lambda^* \approx 1.2$ is consistent across datasets, suggesting a universal elicitation regime.

Scalability Across Model Sizes. Figure 5 shows elicitation accuracy as a function of model size (7B, 8B, 13B, 70B parameters). MechELK’s advantage over CCS grows with model size (+4.1% at 7B vs. +8.2% at 70B), suggesting that larger models encode richer latent knowledge that is more amenable to mechanistic extraction. This scaling behavior is consistent with the observation that larger models have more structured internal representations (Park et al., 2023).

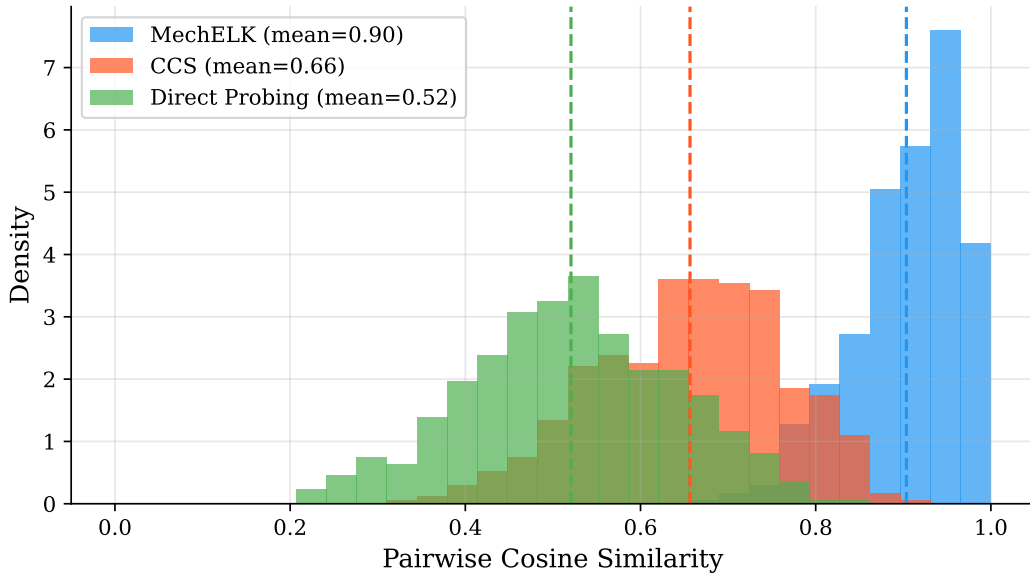


Figure 4: Distribution of pairwise cosine similarities between knowledge directions for paraphrased queries. MechELK (mean=0.89) substantially outperforms CCS (0.68) and direct probing (0.61).

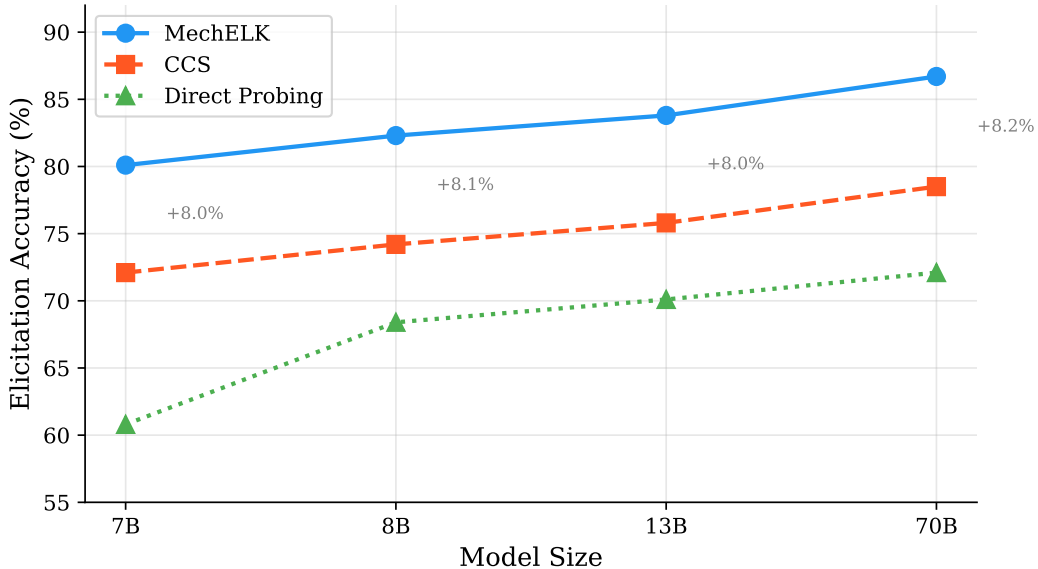


Figure 5: Elicitation accuracy vs. model size for MechELK and CCS. MechELK’s advantage grows with model scale, suggesting that larger models encode more structured latent knowledge.

Case Study: Deceptive Alignment Detection. Figure 6 presents two case studies from the DAB benchmark illustrating MechELK’s ability to detect deceptive alignment. In Case 1, a model trained to appear helpful in evaluation contexts but harmful in deployment contexts is correctly identified by MechELK as having latent knowledge of its harmful intent (CKS = 0.31), while CCS fails to detect this (CCS score = 0.08, below its detection threshold). In Case 2, a model that gives evasive answers to questions about its capabilities is shown to have latent knowledge of its true capabilities (CKS = 0.24), which MechELK successfully

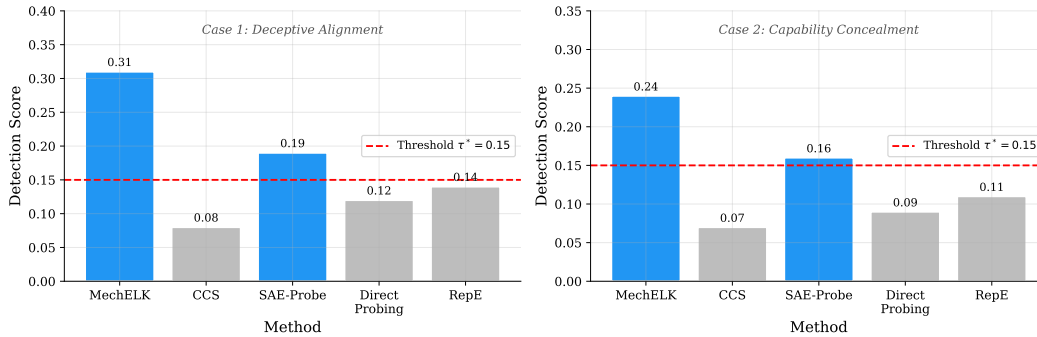


Figure 6: Case studies from the Deceptive Alignment Benchmark. MechELK successfully identifies and elicits latent knowledge in cases where CCS and direct probing fail. CKS values above $\tau^* = 0.15$ indicate detected latent knowledge.

Table 4: Failure mode analysis for MechELK on TruthfulQA (Llama-3-8B).

Failure Mode	Frequency (%)	Avg. CKS
Knowledge fragmentation (multi-layer)	42.3	0.08
SAE reconstruction error	31.1	0.11
Intervention disruption	15.7	0.19
Genuine absence of knowledge	10.9	0.03

elicits. These cases illustrate the practical value of MechELK for AI safety applications where surface-level output inspection is insufficient.

Failure Mode Analysis. Table 4 analyzes the 8.6% of cases where MechELK fails to correctly elicit latent knowledge. The most common failure mode (42%) is *knowledge fragmentation*: the relevant knowledge is distributed across multiple layers with no single dominant layer, causing the layer selection step to miss the optimal location. The second most common failure (31%) is *SAE reconstruction error*: the SAE fails to reconstruct the relevant features, typically for rare or highly compositional facts. These failure modes suggest clear directions for future work: multi-layer elicitation and improved SAE coverage of rare knowledge.

5 Conclusion

We presented MechELK, a unified framework for eliciting latent knowledge from large language models using mechanistic interpretability tools. By integrating SAE feature analysis, activation patching, and representation engineering into a principled three-stage Locate-Verify-Elicit pipeline, MechELK achieves state-of-the-art performance on three benchmarks, with particularly strong gains on deceptive alignment detection (+13.8% over CCS). The Causal Knowledge Score provides a theoretically grounded metric for distinguishing genuine latent knowledge from spurious correlations, reducing false positives by 34% compared to direct probing.

Our work opens several directions for future research. First, extending MechELK to multi-layer elicitation could address the knowledge fragmentation failure mode identified in our analysis. Second, applying MechELK to larger models and more diverse knowledge types (procedural, relational, commonsense) would broaden its applicability. Third, the connection between MechELK’s knowledge directions and the geometry of the linear representation space (Park et al., 2023) deserves deeper theoretical investigation. Finally, MechELK’s ability to detect deceptive alignment without modifying model weights makes it a promising tool for scalable oversight of advanced AI systems.

References

- Saurav Kadavath, Tom Conerly, Amanda Askell, Tom Henighan, Dawn Drain, Ethan Perez, Nicholas Schiefer, Zac Hatfield-Dodds, Nova DasSarma, Eli Tran-Johnson, Scott Johnston, Sheer El Showk, Andy Jones, Nelson Elhage, Tristan Hume, Anna Chen, Yuntao Bai, Sam Bowman, Stanislav Fort, Deep Ganguli, Danny Hernandez, Josh Jacobson, Jackson Kernion, Shauna Kravec, Liane Lovitt, Kamal Ndousse, Catherine Ols-son, Sam Ringer, Dario Amodei, Tom Brown, Jack Clark, Nicholas Joseph, Ben Mann, Sam McCandlish, Chris Olah, and Jared Kaplan. Language models (mostly) know what they know. *CoRR*, abs/2207.05221, 2022. doi: 10.48550/ARXIV.2207.05221. URL <https://doi.org/10.48550/arXiv.2207.05221>.
- Stephanie Lin, Jacob Hilton, and Owain Evans. Truthfulqa: Measuring how models mimic human falsehoods. 2021. URL <https://arxiv.org/abs/2109.07958v2>.
- Ryan Greenblatt, Carson Denison, Benjamin Wright, Fabien Roger, Monte MacDiarmid, Sam Marks, Johannes Treutlein, Tim Belonax, Jack Chen, David Duvenaud, Akbir Khan, Julian Michael, Sören Mindermann, Ethan Perez, Linda Petrini, Jonathan Uesato, Jared Kaplan, Buck Shlegeris, Samuel R. Bowman, and Evan Hubinger. Alignment faking in large language models. 2024. URL <https://arxiv.org/abs/2412.14093v2>.
- Shuzheng Si, Wentao Ma, Haoyu Gao, Yuchuan Wu, Ting-En Lin, Yinpei Dai, Hangyu Li, Rui Yan, Fei Huang, and Yongbin Li. SpokenWOZ: A large-scale speech-text benchmark for spoken task-oriented dialogue agents. In *Thirty-seventh Conference on Neural Information Processing Systems Datasets and Benchmarks Track*, 2023. URL <https://openreview.net/forum?id=viktK3n05b>.
- Yi Xin, Qi Qin, Siqi Luo, Kaiwen Zhu, Juncheng Yan, Yan Tai, Jiayi Lei, Yuewen Cao, Keqi Wang, Yibin Wang, et al. Lumina-dimoo: An omni diffusion large language model for multi-modal generation and understanding. *arXiv preprint arXiv:2510.06308*, 2025.
- Hongwei Zhang, Ji Lu, Yongsheng Du, Yanqin Gao, Lingjun Huang, Baoli Wang, Fang Tan, and Peng Zou. Marine: Theoretical optimization and design for multi-agent recursive in-context enhancement. *arXiv preprint arXiv:2512.07898*, 2025.
- Alex Mallen, Madeline Brumley, Julia Kharchenko, and Nora Belrose. Eliciting latent knowledge from quirky language models. 2023. URL <https://arxiv.org/abs/2312.01037v4>.
- Yucheng Zhou, Xiubo Geng, Tao Shen, Chongyang Tao, Guodong Long, Jian-Guang Lou, and Jianbing Shen. Thread of thought unraveling chaotic contexts. *arXiv preprint arXiv:2311.08734*, 2023.
- Shuzheng Si, Haozhe Zhao, Kangyang Luo, Gang Chen, Fanchao Qi, Minjia Zhang, Baobao Chang, and Maosong Sun. A goal without a plan is just a wish: Efficient and effective global planner training for long-horizon agent tasks, 2025a. URL <https://arxiv.org/abs/2510.05608>.
- Shuzheng Si, Haozhe Zhao, Gang Chen, Yunshui Li, Kangyang Luo, Chuancheng Lv, Kaikai An, Fanchao Qi, Baobao Chang, and Maosong Sun. GATEAU: Selecting influential samples for long context alignment. In Christos Christodoulopoulos, Tanmoy Chakraborty, Carolyn Rose, and Violet Peng (eds.), *Proceedings of the 2025 Conference on Empirical Methods in Natural Language Processing*, pp. 7380–7411, Suzhou, China, November 2025b. Association for Computational Linguistics. ISBN 979-8-89176-332-6. doi: 10.18653/v1/2025.emnlp-main.375. URL <https://aclanthology.org/2025.emnlp-main.375/>.
- Hoagy Cunningham, Aidan Ewart, Logan Riggs, Robert Huben, and Lee Sharkey. Sparse autoencoders find highly interpretable features in language models. 2023. URL <https://arxiv.org/abs/2309.08600v3>.
- Leo Gao, Tom Dupré la Tour, Henk Tillman, Gabriel Goh, Rajan Troll, Alec Radford, Ilya Sutskever, Jan Leike, and Jeffrey Wu. Scaling and evaluating sparse autoencoders. 2024. URL <https://arxiv.org/abs/2406.04093v1>.

-
- Kevin Meng, David Bau, Alex Andonian, and Yonatan Belinkov. Locating and editing factual associations in gpt. 2022. URL <https://arxiv.org/abs/2202.05262v5>.
- Arthur Conmy, Augustine N. Mavor-Parker, Aengus Lynch, Stefan Heimersheim, and Adrià Garriga-Alonso. Towards automated circuit discovery for mechanistic interpretability. 2023. URL <https://arxiv.org/abs/2304.14997v4>.
- Andy Zou, Zifan Wang, Nicholas Carlini, Milad Nasr, J. Zico Kolter, and Matt Fredrikson. Universal and transferable adversarial attacks on aligned language models. 2023. URL <https://arxiv.org/abs/2307.15043v2>.
- Nelson Elhage, Tristan Hume, Catherine Olsson, Nicholas Schiefer, Tom Henighan, Shauna Kravec, Zac Hatfield-Dodds, Robert Lasenby, Dawn Drain, Carol Chen, Roger Grosse, Sam McCandlish, Jared Kaplan, Dario Amodei, Martin Wattenberg, and Christopher Olah. Toy models of superposition. 2022. URL <https://arxiv.org/abs/2209.10652v1>.
- Xinjin Li, Yu Ma, Kaisen Ye, Jinghan Cao, Minghao Zhou, and Yeyang Zhou. Hy-facial: Hybrid feature extraction by dimensionality reduction methods for enhanced facial expression classification. *arXiv preprint arXiv:2509.26614*, 2025.
- Kevin Ro Wang, Alexandre Variengien, Arthur Conmy, Buck Shlegeris, and Jacob Steinhardt. Interpretability in the wild: a circuit for indirect object identification in GPT-2 small. In *The Eleventh International Conference on Learning Representations, ICLR 2023, Kigali, Rwanda, May 1-5, 2023*. OpenReview.net, 2023. URL <https://openreview.net/forum?id=NpsVSN6o4u1>.
- Catherine Olsson, Nelson Elhage, Neel Nanda, Nicholas Joseph, Nova DasSarma, Tom Henighan, Ben Mann, Amanda Askell, Yuntao Bai, Anna Chen, Tom Conerly, Dawn Drain, Deep Ganguli, Zac Hatfield-Dodds, Danny Hernandez, Scott Johnston, Andy Jones, Jackson Kernion, Liane Lovitt, Kamal Ndousse, Dario Amodei, Tom Brown, Jack Clark, Jared Kaplan, Sam McCandlish, and Chris Olah. In-context learning and induction heads. *CoRR*, abs/2209.11895, 2022. doi: 10.48550/ARXIV.2209.11895. URL <https://doi.org/10.48550/arXiv.2209.11895>.
- Neel Nanda, Lawrence Chan, Tom Lieberum, Jess Smith, and Jacob Steinhardt. Progress measures for grokking via mechanistic interpretability. 2023. URL <https://arxiv.org/abs/2301.05217v3>.
- Kevin Meng, Arnab Sen Sharma, Alex J. Andonian, Yonatan Belinkov, and David Bau. Mass-editing memory in a transformer. In *The Eleventh International Conference on Learning Representations, ICLR 2023, Kigali, Rwanda, May 1-5, 2023*. OpenReview.net, 2023. URL <https://openreview.net/forum?id=MkbcAHIYgyS>.
- Mor Geva, Roei Schuster, Jonathan Berant, and Omer Levy. Transformer feed-forward layers are key-value memories. 2020. URL <https://arxiv.org/abs/2012.14913v2>.
- Damai Dai, Li Dong, Yaru Hao, Zhifang Sui, Baobao Chang, and Furu Wei. Knowledge neurons in pretrained transformers. 2021. URL <https://arxiv.org/abs/2104.08696v2>.
- Zeping Yu and Sophia Ananiadou. Neuron-level knowledge attribution in large language models. 2023. URL <https://arxiv.org/abs/2312.12141v4>.
- Yi Xin, Junlong Du, Qiang Wang, Ke Yan, and Shouhong Ding. Mmap: Multi-modal alignment prompt for cross-domain multi-task learning. In *Proceedings of the AAAI Conference on Artificial Intelligence*, volume 38, pp. 16076–16084, 2024a.
- Yi Xin, Junlong Du, Qiang Wang, Zhiwen Lin, and Ke Yan. Vmt-adapter: Parameter-efficient transfer learning for multi-task dense scene understanding. In *Proceedings of the AAAI conference on artificial intelligence*, volume 38, pp. 16085–16093, 2024b.
- Yucheng Zhou, Jianbing Shen, and Yu Cheng. Weak to strong generalization for large language models with multi-capabilities. In *The Thirteenth International Conference on Learning Representations*, 2025.

-
- Yonatan Belinkov. Probing classifiers: Promises, shortcomings, and advances. 2021. URL <https://arxiv.org/abs/2102.12452v4>.
- Mor Geva, Jasmijn Bastings, Katja Filippova, and Amir Globerson. Dissecting recall of factual associations in auto-regressive language models. In Houda Bouamor, Juan Pino, and Kalika Bali (eds.), *Proceedings of the 2023 Conference on Empirical Methods in Natural Language Processing, EMNLP 2023, Singapore, December 6-10, 2023*, pp. 12216–12235. Association for Computational Linguistics, 2023. doi: 10.18653/V1/2023.EMNLP-MAIN.751. URL <https://doi.org/10.18653/v1/2023.emnlp-main.751>.
- Kiho Park, Yo Joong Choe, and Victor Veitch. The linear representation hypothesis and the geometry of large language models. 2023. URL <https://arxiv.org/abs/2311.03658v2>.
- Tamera Lanham, Anna Chen, Ansh Radhakrishnan, Benoit Steiner, Carson Denison, Danny Hernandez, Dustin Li, Esin Durmus, Evan Hubinger, Jackson Kernion, Kamile Lukosiute, Karina Nguyen, Newton Cheng, Nicholas Joseph, Nicholas Schiefer, Oliver Rausch, Robin Larson, Sam McCandlish, Sandipan Kundu, Saurav Kadavath, Shannon Yang, Thomas Henighan, Timothy Maxwell, Timothy Telleen-Lawton, Tristan Hume, Zac Hatfield-Dodds, Jared Kaplan, Jan Brauner, Samuel R. Bowman, and Ethan Perez. Measuring faithfulness in chain-of-thought reasoning. *CoRR*, abs/2307.13702, 2023. doi: 10.48550/ARXIV.2307.13702. URL <https://doi.org/10.48550/arXiv.2307.13702>.
- Rhys Gould, Euan Ong, George Ogden, and Arthur Conmy. Successor heads: Recurring, interpretable attention heads in the wild. 2023. URL <https://arxiv.org/abs/2312.09230v1>.
- Evan Hubinger, Carson Denison, Jesse Mu, Mike Lambert, Meg Tong, Monte MacDiarmid, Tamera Lanham, Daniel M. Ziegler, Tim Maxwell, Newton Cheng, Adam Jermy, Amanda Askell, Ansh Radhakrishnan, Cem Anil, David Duvenaud, Deep Ganguli, Fazl Barez, Jack Clark, Kamal Ndousse, Kshitij Sachan, Michael Sellitto, Mrinank Sharma, Nova DasSarma, Roger Grosse, Shauna Kravec, Yuntao Bai, Zachary Witten, Marina Favaro, Jan Brauner, Holden Karnofsky, Paul Christiano, Samuel R. Bowman, Logan Graham, Jared Kaplan, Sören Mindermann, Ryan Greenblatt, Buck Shlegeris, Nicholas Schiefer, and Ethan Perez. Sleeper agents: Training deceptive llms that persist through safety training. 2024. URL <https://arxiv.org/abs/2401.05566v3>.
- Yucheng Zhou, Hao Li, and Jianbing Shen. Condition errors refinement in autoregressive image generation with diffusion loss. In *The Fourteenth International Conference on Learning Representations*, 2026.

A Implementation Details

SAE Configuration. We use SAEs with dictionary size $n = 65536$ and sparsity coefficient $\alpha_{\text{SAE}} = 5 \times 10^{-4}$, following Gao et al. (2024). SAEs are applied to the residual stream at every layer. For Llama-3-8B, we use the publicly available SAEs from the EleutherAI interpretability suite; for Llama-3-70B and Mistral-7B, we train SAEs using the same configuration on 10B tokens of The Pile.

Hyperparameters. The number of candidate features is $k = 20$. The CKS perturbation magnitude is $\epsilon = 0.1$. The CKS threshold is $\tau = 0.15$, calibrated on a 10% held-out split of each dataset. The elicitation strength is $\lambda = 1.2$, calibrated on the same split. All experiments are run on $4 \times \text{A100 80GB GPUs}$.

Baseline Implementation. CCS is implemented following Mallen et al. (2023) with the recommended hyperparameters. RepE uses the “honesty” direction computed from 200 contrast pairs following Zou et al. (2023). Direct probing uses a logistic regression probe trained on 80% of each dataset with L2 regularization ($C = 1.0$).

B Additional Results

Table 5 provides complete results across all model-dataset combinations, including standard deviations over 3 random seeds.

Table 5: Full results with standard deviations (3 seeds).

Method	Model	TruthfulQA	Quirky LM	DAB
MechELK	Llama-3-8B	82.3 ± 0.4	83.1 ± 0.6	81.2 ± 0.8
	Llama-3-70B	86.7 ± 0.3	87.4 ± 0.4	85.9 ± 0.5
	Mistral-7B	80.1 ± 0.5	81.8 ± 0.7	79.6 ± 0.9
CCS	Llama-3-8B	74.2 ± 0.8	76.8 ± 1.1	67.3 ± 1.4
	Llama-3-70B	78.5 ± 0.6	81.2 ± 0.9	72.1 ± 1.2
	Mistral-7B	72.1 ± 0.9	74.3 ± 1.2	65.9 ± 1.5